NASA Technical Memorandum 4519

Approximate Green's Function Methods for HZE Transport in Multilayered Materials

John W. Wilson, Francis F. Badavi,
Judy L. Shinn, and Robert C. Costen

OCTOBER 1993

NASA Technical Memorandum 4519

Approximate Green's Function Methods for HZE Transport in Multilayered Materials

John W. Wilson
Langley Research Center
Hampton, Virginia

Francis F. Badavi
Christopher Newport University
Newport News, Virginia

Judy L. Shinn and Robert C. Costen
Langley Research Center
Hampton, Virginia

Abstract

A nonperturbative analytic solution of the high charge and energy (HZE) Green's function is used to implement a computer code for laboratory ion beam transport in multilayered materials. The code is established to operate on the Langley nuclear fragmentation model used in engineering applications. Computational procedures are established to generate linear energy transfer (LET) distributions for a specified ion beam and target for comparison with experimental measurements. The code was found to be highly efficient and compared well with the perturbation approximation.

Introduction

Green's function was identified as the likely means of generating efficient high charge and energy (HZE) shielding codes for space engineering that are capable of being validated in laboratory experiments (ref. 1). A derivation of Green's function as a perturbation series gave promise for the development of a laboratory-validated engineering code (ref. 2), but computational inefficiency provided a major obstacle to the code development (ref. 3). More recently, nonperturbative approximations to the HZE Green's function have shown promise in providing an efficient validated engineering code (refs. 4 and 5). Described in the present report is a laboratory code using a nonperturbative Green's function to derive linear energy transfer (LET) spectra behind multilayered targets for ion beams with Z (charges) ≤ 28 corresponding to the major components of the galactic cosmic ray spectrum.

Green's Function for a Single Medium

We restrict our attention to the multicharged ions (atomic number Z_j and atomic mass A_j) for which the Boltzmann equation may be reduced (ref. 6) to

$$\left[\frac{\partial}{\partial x} - \frac{\partial}{\partial E}\widetilde{S}_j(E) + \sigma_j\right]\phi_j(x,E) = \sum_k \sigma_{jk}\,\phi_k(x,E) \tag{1}$$

where $\phi_j(x,E)$ is the ion flux at x with energy E (in MeV/amu), $\widetilde{S}_j(E)$ is the change in E per unit distance, σ_j is the total macroscopic reaction cross section, and σ_{jk} is the macroscopic cross section for the collision of an ion of type k to produce an ion of type j. The solution to equation (1) is to be found subject to the boundary condition

$$\phi_j(0,E) = f_j(E) \tag{2}$$

which, for laboratory beams, has only one value of j for which $f_j(E)$ is not zero and where $f_j(E)$ is described by a mean energy E_o and energy spread σ such that

$$f_j(E) = \frac{1}{\sqrt{2\pi}\sigma}\exp\left[\frac{-(E-E_o)^2}{2\sigma^2}\right] \tag{3}$$

The usual method of solution is to proceed toward solving equation (1) as a perturbation series (refs. 1 and 6). In practice, the computational requirements limit the usefulness of the technique for deep penetration (ref. 3).

The Green's function (G_{jm}) is introduced as a solution of

$$\left[\frac{\partial}{\partial x} - \frac{\partial}{\partial E}\widetilde{S}_j(E) + \sigma_j\right] G_{jm}(x, E, E_o) = \sum_k \sigma_{jk}\, G_{km}(x, E, E_o) \tag{4}$$

subject to the boundary condition

$$G_{jm}(0, E, E_o) = \delta_{jm}\, \delta(E - E_o) \tag{5}$$

where δ_{jm} is Kronecker's δ and $\delta(E - E_o)$ is Dirac's δ function. The solution to equation (1) is given by superposition as

$$\phi_j(x, E) = \sum_k \int G_{jk}(x, E, E')\; f_k(E')\; dE' \tag{6}$$

If $G_{jk}(x, E, E')$ is known as an algebraic quantity, the evaluation of equation (6) may be accomplished by simple integration techniques, and then the associated errors in numerically solving equation (1) are avoided (ref. 7).

The above equations can be simplified by transforming the energy into the residual range (r_j) as

$$r_j = \int_0^E dE'/\widetilde{S}_j(E') \tag{7}$$

and defining new field functions as

$$\psi_j(x, r_j) = \widetilde{S}_j(E)\; \phi_j(x, E) \tag{8}$$

$$\mathcal{G}_{jm}(x, r_j, r'_m) = \widetilde{S}_j(E)\; G_{jm}(x, E, E') \tag{9}$$

$$\hat{f}_j(r_j) = \widetilde{S}_j(E)\; f_j(E) \tag{10}$$

Thus, equation (4) becomes

$$\left(\frac{\partial}{\partial x} - \frac{\partial}{\partial r_j} + \sigma_j\right) \mathcal{G}_{jm}(x, r_j, r'_m) = \sum_k \frac{\nu_j}{\nu_k}\sigma_{jk}\, \mathcal{G}_{km}(x, r_k, r'_m) \tag{11}$$

with the boundary condition

$$\mathcal{G}_{jm}(0, r_j, r'_m) = \delta_{jm}\delta(r_j - r'_m) \tag{12}$$

and with the solution to the ion fields given by

$$\psi_j(x, r_j) = \sum_m \int_0^\infty \mathcal{G}_{jm}(x, r_j, r'_m)\; \hat{f}_m(r'_m)\; dr'_m \tag{13}$$

Note that ν_j, which is the range scale factor as $\nu_j r_j = \nu_m r_m$, is taken as $\nu_j = Z_j^2/A_j$. The solution to equation (11) is written as a perturbation series

$$\mathcal{G}_{jm}(x, r_j, r'_m) = \sum_i \mathcal{G}_{jm}^{(i)}(x, r_j, r'_m) \tag{14}$$

in which

$$\mathcal{G}_{jm}^{(0)}\left(x, r_j, r'_m\right) = g\left(j\right)\ \delta_{jm}\,\delta\left(x + r_j - r'_m\right) \tag{15}$$

and

$$\mathcal{G}_{jm}^{(1)}\left(x, r_j, r'_m\right) \approx \frac{\nu_j \sigma_{jm}\ g\left(j, m\right)}{x\left(\nu_m - \nu_j\right)} \tag{16}$$

where $\mathcal{G}_{jm}^{(1)}(x, r_j, r'_m)$ is zero unless

$$\frac{\nu_j}{\nu_m}\left(r_j + x\right) \leq r'_m \leq \frac{\nu_j}{\nu_m} r_j + x \tag{17}$$

for $\nu_m > \nu_j$. If $\nu_j > \nu_m$, as can happen in neutron removal, the negative of equation (16) is used and the upper and lower limits of equation (17) are switched. The higher terms are approximated as

$$\mathcal{G}_{jm}^{(i)}\left(x, r_j, r'_m\right) \approx \sum_{k_1, k_2, \ldots, k_{i-1}} \frac{\nu_j \sigma_{jk_1} \sigma_{k_1 k_2}, \cdots, \sigma_{k_{i-1} m}\ g\left(j, k_1, k_2, \cdots, k_{i-1}, m\right)}{x\left(\nu_m - \nu_j\right)} \tag{18}$$

In the above equations,

$$g\left(j\right) = e^{-\sigma_j x} \tag{19}$$

and

$$g\left(j_1, j_2, \ldots, j_n, j_{n+1}\right) = \frac{g\left(j_1, j_2, \ldots, j_{n-1}, j_n\right) - g\left(j_1, j_2, \ldots, j_{n-1}, j_{n+1}\right)}{\sigma_{j_{n+1}} - \sigma_{j_n}} \tag{20}$$

Note that $\mathcal{G}_{jm}^{(i)}(x, r_j, r'_m)$ is purely dependent on x for $i > 0$, which we represent as $\mathcal{G}_{jm}^{(i)}(x)$. (See ref. 3.) In terms of the above, the solution to equation (1) becomes (from ref. 3)

$$\begin{aligned} \psi_j\left(x, r_j\right) &= e^{-\sigma_j x}\,\hat{f}_j\left(r_j + x\right) \\ &\quad + \sum_{m,i} \mathcal{G}_{jm}^{(i)}\left(x\right)\left[\widehat{F}_m\left(r'_{m\ell}\right) - \widehat{F}_m\left(r'_{mu}\right)\right] \end{aligned} \tag{21}$$

In equation (21), r'_{mu} and $r'_{m\ell}$ are given by the upper and lower limits of the inequality of equation (17). The symbol $\widehat{F}_m(r'_m)$ refers to the integral spectrum

$$\widehat{F}_m\left(r'_m\right) = \int_{r'_m}^{\infty} \hat{f}_m\left(r\right)\ dr \tag{22}$$

We note that

$$\widehat{F}_m\left(r'_m\right) \equiv F_m\left(E'\right) \tag{23}$$

with

$$F_m\left(E'\right) = \int_{E'}^{\infty} f_m\left(E\right)\ dE \tag{24}$$

and

$$r'_m = \int_0^{E'} dE / \widetilde{S}_m(E) \tag{25}$$

We now introduce nonperturbative terms for the summation in equation (21).

First, we recall that the g function of n arguments was generated by the perturbation solution of the transport equation neglecting ionization energy loss (ref. 1) given by

$$\left[\frac{\partial}{\partial x} + \sigma_j\right] g_{jm}(x) = \sum_k \sigma_{jk}\, g_{km}(x) \tag{26}$$

subject to the boundary condition

$$g_{jm}(0) = \delta_{jm} \tag{27}$$

for which the solution is

$$g_{jm}(x) = \delta_{jm}\, g(m) + \sigma_{jm}\, g(j,m) + \cdots \tag{28}$$

It is also true that

$$g_{jm}(x) = \sum_k g_{jk}(x-y)\, g_{km}(y) \tag{29}$$

for any positive values of x and y. Equation (29) may be used to propagate the function $g_{jm}(x)$ over the solution space after which

$$\mathcal{G}_{jm}(x, r_j, r'_m) \approx e^{-\sigma_j x}\delta_{jm}\,\delta(x + r_j - r'_m) + \frac{\nu_j\left[g_{jm}(x) - e^{-\sigma_j x}\delta_{jm}\right]}{x(\nu_m - \nu_j)} \tag{30}$$

The approximate solution of equation (1) is then given by

$$\psi_j(x, r_j) \approx e^{-\sigma_j x}\,\hat{f}(r_j + x) + \sum_m \frac{\nu_j\left[g_{jm}(x) - e^{-\sigma_j x}\delta_{jm}\right]}{x(\nu_m - \nu_j)}\left[\widehat{F}_m(r'_{mu}) - \widehat{F}_m(r'_{m\ell})\right] \tag{31}$$

which is a relatively simple quantity (ref. 4).

Green's Function in a Shielded Medium

The major simplification in the Green's function method results from the fact that the scaled spectral distribution of secondary ions to a first approximation depends only on the depth of penetration as seen in equations (16), (18), and (30). Our first approach to a multilayered Green's function will rely on this observation and assume its validity for multilayered shields.

If we consider a domain labeled as "1" that is shielded by a second domain labeled as "2," the number of type j ions at depth x in 1 due to type m ions incident on domain 2 of thickness y is

$$g_{12\,jm}(x, y) = \sum_k g_{1jk}(x)\, g_{2km}(y) \tag{32}$$

The leading term in equation (32) is the penetrating primaries as

$$g_{12jm}(x,y) = e^{-\sigma_{1j}x-\sigma_{2j}y}\delta_{jm} + \left[g_{12jm}(x,y) - e^{-\sigma_{1j}x-\sigma_{2j}y}\delta_{jm}\right] \tag{33}$$

in which all higher order terms are within the brackets of equation (33).

The first term of the scaled Green's function is then

$$\mathcal{G}^{(0)}_{12jm}(x,y,r_j,r'_m) = e^{-\sigma_{1j}x-\sigma_{2j}y}\delta_{jm}\,\delta\left[x + r_j - (r'_m - \rho y)\right] \tag{34}$$

in which ρ is the range scale factor for the two media

$$\rho = \frac{R_{1j}(E)}{R_{2j}(E)} \tag{35}$$

The ratio of range in water to range in aluminum for proton beams (eq. (35)) is shown in sketch A. We take a single value for ρ corresponding to 600 MeV/amu. The secondary contribution is similarly found by noting that equation (17) becomes

$$\frac{\nu_j}{\nu_m}(r_j + x + \rho y) \le r'_m \le \frac{\nu_j}{\nu_m} r_j + x + \rho y \tag{36}$$

from which the average spectrum is evaluated. The full approximate Green's function is then

$$\begin{aligned}\mathcal{G}_{12jm}(x,y,r_j,r'_m) \approx\ & e^{-\sigma_{1j}x-\sigma_{2j}y}\delta_{jm}\,\delta\left(x + \rho y + r_j - r'_m\right) \\ & + \frac{\nu_j\left[g_{12jm}(x,y) - e^{-\sigma_{1j}x-\sigma_{2j}y}\delta_{jm}\right]}{(x+\rho y)(\nu_m - \nu_j)}\end{aligned} \tag{37}$$

Equation (37) is our first approximation to the Green's function in a shielded medium (two layers) and is easily modified to multilayers. We now consider the first spectral modification.

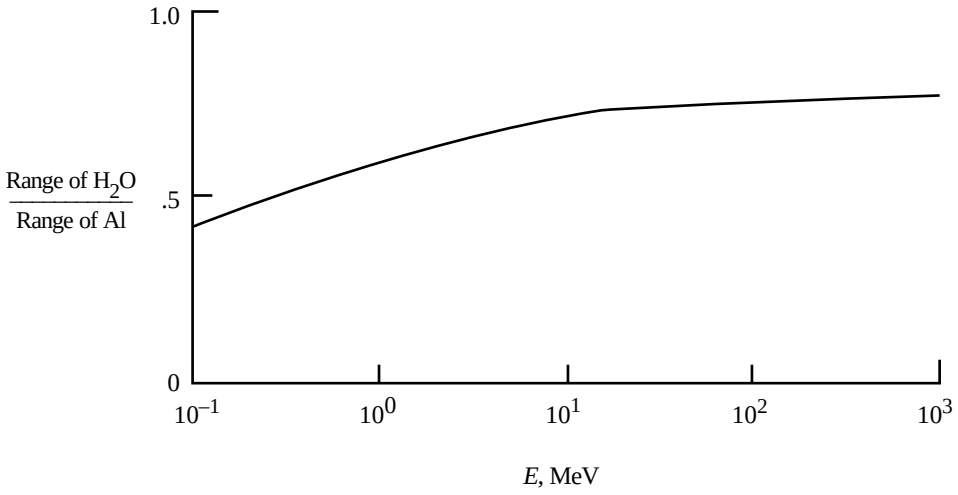

Sketch A

Showing that the first collision term has the properties

$$\mathcal{G}^{(1)}_{12jm}\left(x,y,r_j,r'_m\right)=\left\{\begin{array}{ll}\dfrac{\nu_j\sigma_{1jm}e^{-\sigma_{1m}x-\sigma_{2m}y}}{\left|\nu_m-\nu_j\right|} & \left(r'_m=r'_{mu}\right)\\ \dfrac{\nu_j\sigma_{2jm}e^{-\sigma_{1j}x-\sigma_{2j}y}}{\left|\nu_m-\nu_j\right|} & \left(r'_m=r'_{m\ell}\right)\end{array}\right\} \tag{38}$$

is easy; we use these properties to derive a simple correction for the average spectrum as

$$\mathcal{G}^{(1)}_{12jm}\left(x,y,r_j,r'_m\right)=\frac{\nu_j\ g^{(1)}_{12jm}\left(x,y\right)}{\left(x+\rho y\right)\left(\nu_m-\nu_j\right)}+b_{jm}\left(x,y\right)\left(r'_m-\bar{r}_m\right) \tag{39}$$

where $g^{(1)}_{12jm}(x,y)$ is the first collision term of equation (39) and

$$\bar{r}'_m=\frac{r'_{mu}+r'_{m\ell}}{2} \tag{40}$$

is the midpoint of $\bar{r}'_m$ between its limits given by equation (36). The b_{jm} term of equation (39) has the property that

$$\int_{r'_{m\ell}}^{r'_{mu}} b_{jm}\left(x,y\right)\ \left(r'-\bar{r}'_m\right)\ dr'=0 \tag{41}$$

thus ensuring that the first term of equation (39) is, indeed, the average spectrum as required. The spectral slope parameter is found to be

$$b_{jm}\left(x,y\right)=\frac{\nu_j\nu_m\left(\sigma_{1jm}e^{-\sigma_{1m}x-\sigma_{2m}y}-\sigma_{2jm}e^{-\sigma_{1j}x-\sigma_{2j}y}\right)}{\left(x+\rho y\right)\left(\nu_m-\nu_j\right)\left|\nu_m-\nu_j\right|} \tag{42}$$

A similarly simple spectral correction can be made to the higher order terms. The spectral correction given in equation (42) will be included in the present Green's function code.

LET Spectra for Laboratory Beams

We use the boundary condition appropriate for laboratory beams given by equation (3). The cumulative spectrum is given by

$$F_j\left(E\right)=\frac{1}{2}\left[1-\mathrm{erf}\left(\frac{E-E_o}{\sqrt{2}\sigma}\right)\right] \tag{43}$$

The cumulative energy moment needed to evaluate the spectral correction is

$$\overline{E}_j\left(E\right)=\frac{1}{2}E_o\left[1-\mathrm{erf}\left(\frac{E-E_o}{\sqrt{2}\sigma}\right)\right]+\frac{\sigma}{\sqrt{2\pi}}\exp\left[-\frac{\left(E-E_o\right)^2}{2\sigma^2}\right] \tag{44}$$

The average energy on any subinterval (E_1,E_2) is then

$$\overline{E}=\frac{\overline{E}_j\left(E_1\right)-\overline{E}_j\left(E_2\right)}{F_j\left(E_1\right)-F_j\left(E_2\right)} \tag{45}$$

The beam-generated flux is

$$\psi_j(x,y,r_j) = e^{-\sigma_{1j}x-\sigma_{2j}y}\hat{f}_j(r_j+x+\rho y) + \sum_{m,i}\mathcal{G}_{jm}^{(i)}(x,y)\left[\widehat{F}_m(r'_{mu}) - \widehat{F}_m(r'_{m\ell})\right] + \sum_m b_{jm}^{(1)}(x,y)\left[r'_m(\overline{E}) - \bar{r}'_m\right]\left[\widehat{F}_m(r'_{mu}) - \widehat{F}_m(r'_{m\ell})\right] \quad (46)$$

where $\overline{E}$ is evaluated using equation (45) with E_1 and E_2 as the lower and upper limits associated with $r'_{m\ell}$ and r'_{mu}, respectively.

The differential fluence spectra for a 600-MeV/amu ^{56}Fe beam with a 2.5-MeV/amu standard deviation incident on a water slab are shown in figure 1. A single layer of 5 cm of water is shown in figure 1(a) and a double layer of 2.5 cm of water followed by 2.5 cm of water is shown in figure 1(b). A consistency check is performed on the multilayered code by comparing it with the single-layered computation when the two layers are of the same size and composition. The ratio of multilayered results to single-layered results differs by less than ± 1 percent. The LET distribution is found by using the methods of reference 8. The corresponding LET spectra are shown in figure 2. The highest LET peak is due to the primary beam and the iron fragments. The successive peaks below iron are due to lower atomic weight fragments. The lowest LET peak consists of relativistic charge fragments of p, d, and t particles that are produced in abundance in HZE collisions (ref. 9). The peak near 10 MeV/cm consists of he- and α-particles that are also produced abundantly. Many of the HZE fragments are produced with a charge near the projectile charge, as Shinn, Townsend, and Wilson found earlier for hydrogenic targets (ref. 10). Note that no distinguishable difference exists between the LET spectra of the single-layered code (fig. 2(a)) and the multilayered code (fig. 2(b)) at the same penetration depth in water, which further demonstrates code consistency.

A series of evaluations for a (2.24-g/cm^2) lead-scattering foil is shown in figure 3. The lead-scattering foil is usually part of the accelerator beam line (at the Lawrence Berkeley Laboratory Bevalac accelerator) with the result that the fragments from the lead target are seen as contamination. Clearly, these fragments must be modeled to properly interpret the attenuation of the beam in the water target in actual experiments. The corresponding LET spectra at various depths of a water target are shown in figure 4. The importance of the fragmentation in the scattering foil is seen in comparing figure 4(a) with figure 4(b). Note that fewer of the fragmentations result in fragments near the beam charge for the lead foil in comparison with the water target, as seen by comparing the relative magnitudes of the three highest LET peaks in figures 2(a) and 4(a). These differences are part of the reason why hydrogenic targets are important to space radiation protection. At greater depths the LET distributions begin to overlap, and distinguishing the different charge groups becomes more difficult. Such LET spectra will be compared with experimental measurements in the near future.

Concluding Remarks

A formalism for the evaluation of Green's function in multilayered target configurations has been derived and a computer code generated. The code satisfies a consistency check for multilayered-material calculations when the layers are of uniform composition by comparing the results with the single-layered code. The importance of the multilayered code in the analysis of

experimental ion beams has been shown by demonstrating the effects of a lead-scattering foil in the Bevalac beam line. An analysis of such experiments is in progress.

NASA Langley Research Center
Hampton, VA 23681-0001
September 10, 1993

References

1. Wilson, J. W.; Lamkin, Stanley L.; Farhat, Hamidullah; Ganapol, Barry D.; and Townsend, Lawrence W.: *A Hierarchy of Transport Approximations for High Energy Heavy (HZE) Ions.* NASA TM-4118, 1989.

2. Wilson, John W.; Townsend, L. W.; Lamkin, S. L.; and Ganapol, B. D.: A Closed-Form Solution to HZE Propagation. *Radiat. Res.*, vol. 122, 1990, pp. 223–228.

3. Wilson, J. W.; and Badavi, F. F.: New Directions in Heavy Ion Shielding. *Proceedings of the Topical Meeting on New Horizons in Radiation Protection and Shielding*, American Nucl. Soc., Inc., 1992, pp. 205–211.

4. Wilson, John W.; Costen, Robert C.; Shinn, Judy L.; and Badavi, Francis F.: *Green's Function Methods in Heavy Ion Shielding.* NASA TP-3311, 1993.

5. Wilson, John W.; Badavi, Francis F.; Costen, Robert C.; and Shinn, Judy L.: *Nonperturbative Methods for HZE Transport.* NASA TP-3363, 1993.

6. Wilson, John W.: *Analysis of the Theory of High-Energy Ion Transport.* NASA TN D-8381, 1977.

7. Wilson, John W.; Townsend, Lawrence W.; Schimmerling, Walter; Khandelwal, Govind S.; Khan, Ferdous; Nealy, John E.; Cucinotta, Francis A.; Simonsen, Lisa C.; Shinn, Judy L.; and Norbury, John W.: *Transport Methods and Interactions for Space Radiations.* NASA RP-1257, 1991.

8. Wilson, John W.; and Badavi, Francis F.: *A Study of the Generation of Linear Energy Transfer Spectra for Space Radiations.* NASA TM-4410, 1992.

9. Wilson, J. W.; Chun, S. Y.; Badavi, F. F.; and John, S.: *Coulomb Effects in Low-Energy Nuclear Fragmentation.* NASA TP-3352, 1993.

10. Shinn, Judy L.; Townsend, Lawrence W.; and Wilson, John W.: Galactic Cosmic Ray Radiation Levels in Spacecraft on Interplanetary Missions. *Book of Abstracts—The World Space Congress, 43rd Congress of the International Astronautical Federation and 29th Plenary Meeting of the Committee on Space Research*, International Astronautical Federation and Committee on Space Research, Aug.–Sept. 1992, pp. 567–568.

(a) 0 cm of H_2O followed by 5 cm of H_2O.

(b) 2.5 cm of H_2O followed by 2.5 cm of H_2O.

Figure 1. Differential fluence spectra for 600-MeV/amu ^{56}Fe beam with 2.5-MeV/amu standard deviation incident on water slab.

(a) 0 cm of H_2O followed by 5 cm of H_2O.

(b) 2.5 cm of H_2O followed by 2.5 cm of H_2O.

Figure 2. LET distribution for 600-MeV/amu ^{56}Fe beam with 2.5-MeV/amu standard deviation incident on water slab.

(a) 0 cm of H_2O.

(b) 5 cm of H_2O.

Figure 3. Differential fluence for 525-MeV/amu ^{56}Fe beam with 2.5-MeV/amu standard deviation after passing through 2.24-g/cm^2 lead-scattering foil and water target.

(c) 10 cm of H_2O.

Figure 3. Concluded.

(a) 0 cm of H_2O.

(b) 5 cm of H_2O.

Figure 4. LET distribution for 525-MeV/amu ^{56}Fe beam with 2.5-MeV/amu standard deviation after passing through 2.24-g/cm^2 lead-scattering foil and water target.

(c) 10 cm of H_2O.

Figure 4. Concluded.

REPORT DOCUMENTATION PAGE

Form Approved
OMB No. 0704-0188

Public reporting burden for this collection of information is estimated to average 1 hour per response, including the time for reviewing instructions, searching existing data sources, gathering and maintaining the data needed, and completing and reviewing the collection of information. Send comments regarding this burden estimate or any other aspect of this collection of information, including suggestions for reducing this burden, to Washington Headquarters Services, Directorate for Information Operations and Reports, 1215 Jefferson Davis Highway, Suite 1204, Arlington, VA 22202-4302, and to the Office of Management and Budget, Paperwork Reduction Project (0704-0188), Washington, DC 20503.

1. AGENCY USE ONLY *(Leave blank)*	2. REPORT DATE	3. REPORT TYPE AND DATES COVERED
	October 1993	Technical Memorandum

4. TITLE AND SUBTITLE
Approximate Green's Function Methods for HZE Transport in Multilayered Materials

5. FUNDING NUMBERS
WU 199-45-16-11

6. AUTHOR(S)
John W. Wilson, Francis F. Badavi, Judy L. Shinn, and Robert C. Costen

7. PERFORMING ORGANIZATION NAME(S) AND ADDRESS(ES)
NASA Langley Research Center
Hampton, VA 23681-0001

8. PERFORMING ORGANIZATION REPORT NUMBER
L-17302

9. SPONSORING/MONITORING AGENCY NAME(S) AND ADDRESS(ES)
National Aeronautics and Space Administration
Washington, DC 20546-0001

10. SPONSORING/MONITORING AGENCY REPORT NUMBER
NASA TM-4519

11. SUPPLEMENTARY NOTES
Wilson, Shinn, and Costen: Langley Research Center, Hampton, VA; Badavi: Christopher Newport University, Newport News, VA.

12a. DISTRIBUTION/AVAILABILITY STATEMENT
Unclassified–Unlimited

Subject Category 93

12b. DISTRIBUTION CODE

13. ABSTRACT *(Maximum 200 words)*
A nonperturbative analytic solution of the high charge and energy (HZE) Green's function is used to implement a computer code for laboratory ion beam transport in multilayered materials. The code is established to operate on the Langley nuclear fragmentation model used in engineering applications. Computational procedures are established to generate linear energy transfer (LET) distributions for a specified ion beam and target for comparison with experimental measurements. The code was found to be highly efficient and compared well with the perturbation approximation.

14. SUBJECT TERMS
Radiation shielding; Multilayer; Green's function

15. NUMBER OF PAGES
15

16. PRICE CODE
A03

17. SECURITY CLASSIFICATION OF REPORT	18. SECURITY CLASSIFICATION OF THIS PAGE	19. SECURITY CLASSIFICATION OF ABSTRACT	20. LIMITATION OF ABSTRACT
Unclassified	Unclassified		